PAPER *Special Section on Recent Advances in Multimedia Signal Processing Techniques and Applications*

A Correlation-Based Watermarking Technique of 3-D Meshes via Cyclic Signal Processing

Toshiyuki UTO[†a)], ***Member***, **Yuka TAKEMURA**[†*], **Hidekazu KAMITANI**[†], ***Nonmembers***, ***and*** **Kenji OHUE**[†], ***Member***

SUMMARY This paper describes a blind watermarking scheme through cyclic signal processing. Due to various rapid networks, there is a growing demand of copyright protection for multimedia data. As efficient watermarking of images, there exist two major approaches: a quantization-based method and a correlation-based method. In this paper, we proposes a correlation-based watermarking technique of three-dimensional (3-D) polygonal models using the fast Fourier transforms (FFTs). For generating a watermark with desirable properties, similar to a pseudonoise signal, an impulse signal on a two-dimensional (2-D) space is spread through the FFT, the multiplication of a complex sinusoid signal, and the inverse FFT. This watermark, i.e., spread impulse signal, in a transform domain is converted to a spatial domain by an inverse wavelet transform, and embedded into 3-D data aligned by the principle component analysis (PCA). In the detection procedure, after realigning the watermarked mesh model through the PCA, we map the 3-D data on the 2-D space via block segmentation and averaging operation. The 2-D data are processed by the inverse system, i.e., the FFT, the division of the complex sinusoid signal, and the inverse FFT. From the resulting 2-D signal, we detect the position of the maximum value as a signature. For 3-D bunny models, detection rates and information capacity are shown to evaluate the performance of the proposed method.

key words: *watermarking, spread spectrum code, 3-D mesh, cyclic signal processing*

1. Introduction

There has been a significant growth in the field of digital watermarking [1]–[3]. Most previous studies on digital watermarking deal with its application to text data, audio, images, and video. One of image watermarking approaches is spread spectrum technique [4], where the watermark is a pseudonoise signal generated from a secret key. To detect this signature in the watermarked image, a correlation between the pseudonoise signal and the watermarked image is calculated. According to the correlation value, a detector can obtain the embedded message by the correct key. Another image watermarking approach is quantization index modulation (QIM) technique [5], where the watermark is embedded by means of the choice of quantizer. A notable property of QIM-based watermarking is that no secret key is required to embed and detect the watermark. In addition to these popular methods, watermarking algorithms for different media types have been proposed [1]. Watermarking of three-dimensional (3-D) meshes was first introduced in [6], where 3-D meshes include Virtual Reality Modeling Language and computer-aided design. In the recent years, several 3-D watermarking methods have been presented in [7]–[9] to improve the performance in terms of perceptual transparency, robustness and payload of the watermark.

In this paper, we propose a blind watermarking algorithm with the fast Fourier transforms (FFTs) for 3-D polygonal meshes. Similar to the pseudonoise signal in spread spectrum watermarking, we utilize a spread spectrum code as the watermark. For generating the spread spectrum code from an impulse signal, which has a flat frequency response over all frequencies, we employ the following processes: the FFT, the multiplication of a complex sinusoid signal, and the inverse FFT [10]. This implementation for the impulse signal disperses the energy in the spatial domain without modifying the magnitude response, since the system corresponds to an allpass filter in cyclic signal processing [11]. Inverse wavelet transform coefficients of the resulting signal are multiplied by a small gain factor and added to a 3-D mesh. To detect the watermark, both inverse mapping and de-spreading are applied to the watermarked 3-D model. The position of the peak value in the obtained signal results in a detected message. In the proposed watermarking of 3-D meshes, positions of the peak value in the impulse signal and the detected signal play a significant role. For registering a target model with the stego model, we utilize the principle component analysis (PCA) [12], [13] for 3-D mesh models. Finally, we demonstrate the robustness to rotation, translation, scaling, and additive noises, in addition to the subjective performance of the proposed algorithm.

2. Related Work

Various schemes for robust watermarking of 3-D meshes have been proposed in [14]–[16]. It is well known that there exists a complex trade-off between basic requirements, such as data payload, invisibility, robustness and security, for a secure watermark.

In [14], Uccheddu et al. proposed a wavelet-based blind watermarking of 3-D meshes with semi-regular connectivity. Our approach is similar to their approach in that the PCA is employed for achieving robustness against geometric transformations such as rotation, translation and uniform scaling, and a map matrix is used in the embedding phase to insert a watermark. On the other hand, our method dif-

Manuscript received May 2, 2011.
Manuscript revised September 1, 2011.

†The authors are with the Department of Computer Science, Faculty of Engineering, Ehime University, Matsuyama-shi, 790–8577 Japan.
*Presently, with the Ube Information Systems.
a) E-mail: uto@cs.ehime-u.ac.jp

DOI: 10.1587/transinf.E95.D.1272

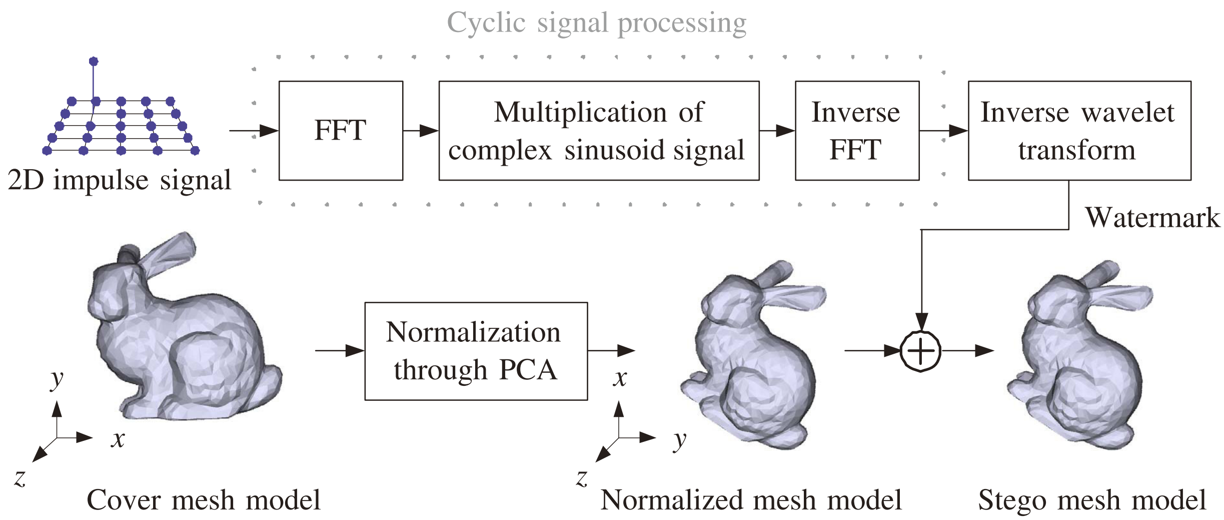

Fig. 1 Block diagram of the watermark embedding for the proposed watermarking method.

fers from their method in the following points. One of the differences is that we utilize a orthogonal sequence, instead of a pseudo-random sequence in [14], as the watermark. Since the pseudo-random sequence is classified into a quasi-orthogonal sequence, the proposed technique is superior to the previous technique. Furthermore, whereas the orthogonal sequence in our method is uniquely calculated, as shown in Sect. 3, the pseudo-random sequence in [14] is stochastically determined via a seed. Another of the differences is that our approach can be applied to arbitrary 3-D meshes, instead of semi-regular meshes. Remeshing algorithms [17]–[19] can transform irregular meshes into semi-regular form, but are a time-consuming procedure and cause error between an original mesh and an approximate mesh with semi-regular connectivity.

In [15], Kanai et al. also introduced an robust watermarking based on the multiresolution wavelet decomposition for 3-D semi-regular meshes. The proposed watermarking algorithm in this paper and the watermarking algorithm in [14] are classified into blind detection systems [2], because additional information concerning the original object is not needed for successful watermark detection. On the other hand, the watermarking algorithm in [15] is categorized into non-blind detection systems. It is obvious that the blind watermark detection is a major advantage, due to the fact that neither original data knowledge nor time consuming search in owners' database is needed.

In [16], Benedens presented two watermarking methods called the vertex flood algorithm and the triangle flood algorithm, where the highest capacity for 3-D meshes is nearly one bit per triangle. Since these methods differ considerably from our method in data payload and employed techniques, it is nontrivial to fairly compare the proposed approach in this paper with [16].

3. Proposed Watermarking Method

In this section, we present a watermarking technique based on cyclic signal processing [11]. This method embeds watermark information into a 3-D polygonal mesh by adding a spread spectrum code generated from an impulse signal on a two-dimensional (2-D) space. The watermark in the stego mesh model is extracted by a correlation-based detector. Both the watermark embedding and extraction processes are described in the following sections.

3.1 Watermark via Cyclic Signal Processing

Figure 1 depicts a block diagram of watermark embedding for 3-D mesh models. In the proposed scheme, we construct the watermark from the 2-D impulse signal. Here, the 2-D impulse signal $s(m,n)$ ($m = 0, 1, \ldots, M-1$, $n = 0, 1, \ldots, N-1$) with a signature message (P, Q) is defined as

$$s(m,n) = \begin{cases} 1, & \text{for } (m,n) = (P,Q), \\ 0, & \text{for } (m,n) \neq (P,Q). \end{cases} \tag{1}$$

For dispersing the energy of the 2-D impulse signal, we employ the following three steps: the FFT, the multiplication of complex sinusoid signal, and the inverse FFT. The output signal $s'(m,n)$ of this implementation is expressed by

$$\mathbf{S}' = \mathbf{A}_M \cdot \mathbf{S} \cdot \mathbf{A}_N^T, \tag{2}$$

$$\mathbf{A}_K = \frac{1}{K}\mathbf{W}_K^{\dagger} \cdot \mathbf{D}_K \cdot \mathbf{W}_K, \tag{3}$$

$$\mathbf{W}_K = \begin{bmatrix} e^{-j2\pi 0\cdot 0/K} & e^{-j2\pi 0\cdot 1/K} \\ e^{-j2\pi 1\cdot 0/K} & e^{-j2\pi 1\cdot 1/K} \\ \vdots & \vdots \\ e^{-j2\pi (K-1)\cdot 0/K} & e^{-j2\pi (K-1)\cdot 1/K} \end{bmatrix}$$

$$\begin{matrix} \cdots & e^{-j2\pi 0\cdot(K-1)/K} \\ \cdots & e^{-j2\pi 1\cdot(K-1)/K} \\ \ddots & \vdots \\ \cdots & e^{-j2\pi(K-1)\cdot(K-1)/K} \end{matrix}\Bigg], \tag{4}$$

$$\mathbf{D}_K = \mathrm{diag}\left(e^{j\theta_{0,K}}, e^{j\theta_{1,K}}, \ldots, e^{j\theta_{K-1,K}}\right), \tag{5}$$

where $\mathbf{S}'$ is the output matrix with the (m,n)-th elements $s'(m,n)$, $\mathbf{S}$ is the input matrix with the (m,n)-th elements $s(m,n)$, $\mathbf{W}_K$ is the $K \times K$ discrete Fourier transform matrix, $\mathbf{D}_K$ is a $K \times K$ diagonal matrix with diagonal entries $e^{j\theta_{k,K}}$ $(k = 0, 1, \ldots, K-1)$, and $\mathbf{B}^T$ and $\mathbf{B}^\dagger$ denote the transpose and the conjugated transpose of matrix $\mathbf{B}$, respectively. Since the $K \times K$ circulant matrix $\mathbf{A}_K$ in Eq. (3) corresponds a cyclic allpass system [11], the magnitude response of $s'(m,n)$ is equivalent to that of the impulse signal $s(m,n)$. Substituting

$$\theta_{k,K} = \begin{cases} \frac{2\pi}{K}\alpha_K\left(k^2 - \frac{K}{2}k\right), \\ \qquad \text{for } k = 0, 1, \ldots, K', \\ -\frac{2\pi}{K}\alpha_K\left((K-k)^2 - \frac{K}{2}(K-k)\right), \\ \qquad \text{for } k = K'+1, K'+2, \ldots, K-1 \end{cases} \tag{6}$$

$$K' = \begin{cases} \frac{K-1}{2}, & \text{for } K \text{ odd} \\ \frac{K}{2}, & \text{for } K \text{ even} \end{cases} \tag{7}$$

into Eq. (5), we can obtain the smear transform in [10], where α_K is a spreading factor. The phase response in Eq. (6) is defined such that the group delay response of the cyclic allpass filter is a linear sequence with respect to k. As a result, the output signal $s'(m,n)$ from this cyclic system with appropriate spreading factor α_K for the impulse response is dispersed on each index (m,n) and increase robustness of the watermark against some common attacks. The idea behind the proposed scheme is similar to spread spectrum schemes with a pseudonoise sequence [2], [4]. For example, when $K = 32$ and $\alpha_K = 5$, an one-dimensional (1-D) impulse signal $s(k)$ $(k = 0, 1, \ldots, K-1)$ with a signature message $P = 0$ and an output signal $s'(k)$ of the cyclic allpass filter for $s(k)$ are illustrated in Fig. 2 (a) and Fig. 2 (b), respectively, where

$$\begin{aligned} &\left[s'(0) \quad s'(1) \quad \cdots \quad s'(K-1)\right]^T \\ &\quad = \mathbf{A}_K \cdot \left[s(0) \quad s(1) \quad \cdots \quad s(K-1)\right]^T \\ &\quad = \mathbf{A}_K \cdot \left[1 \quad 0 \quad \cdots \quad 0\right]. \end{aligned} \tag{8}$$

In addition, Fig. 2 (c) shows the magnitude response of $s'(k)$, which is same as that of $s(k)$.

For the conversion from a transform domain to a spatial domain, we employ a inverse wavelet transform. When the spread information $s'(m,n)$ are embedded in the HH band of the Haar wavelet, a watermark $w(m',n')$ $(m' = 0, 1, \ldots, 2M-1,\ n' = 0, 1, \ldots, 2N-1)$ in the spatial domain is expressed as

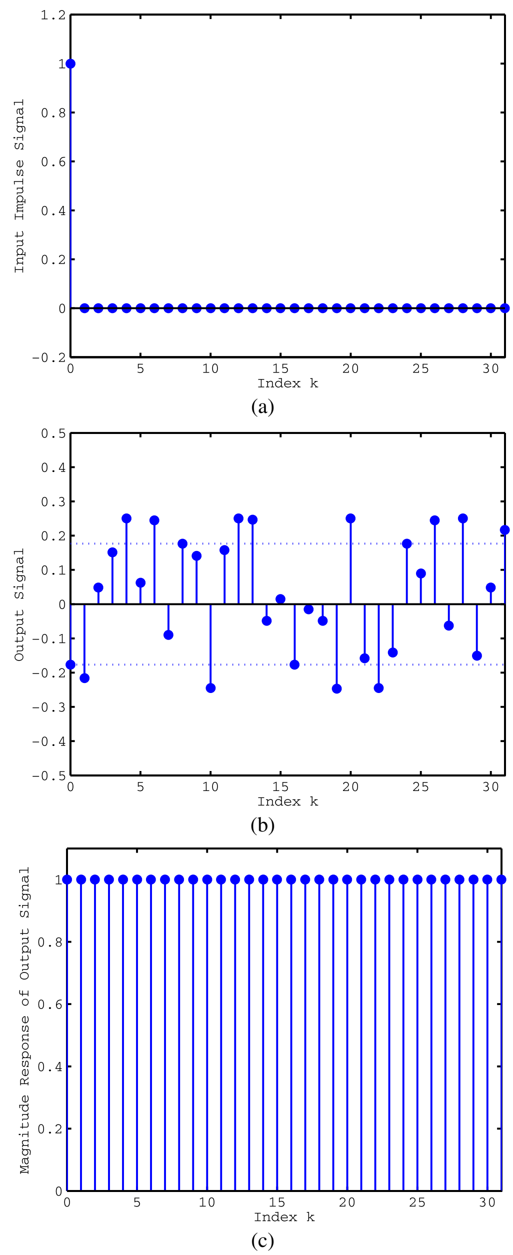

Fig. 2 Example of spread spectrum code in (1): (a) input impulse signal $s(k)$, (b) output signal $s'(k)$, and (c) magnitude response of $s'(k)$.

$$w(m',n') = \begin{cases} s'(m'/2, n'/2)/2, \\ \qquad \text{for } m' \text{ even and } n' \text{ even}, \\ -s'((m'-1)/2, n'/2)/2, \\ \qquad \text{for } m' \text{ odd and } n' \text{ even}, \\ -s'(m'/2, (n'-1)/2)/2, \\ \qquad \text{for } m' \text{ even and } n' \text{ odd}, \\ s'((m'-1)/2, (n'-1)/2)/2, \\ \qquad \text{for } m' \text{ odd and } n' \text{ odd}. \end{cases} \tag{9}$$

In this paper, we generate two watermarks $w_c(m',n')$ $(c \in \{y,z\})$ via the aforementioned algorithm for 3-D meshes.

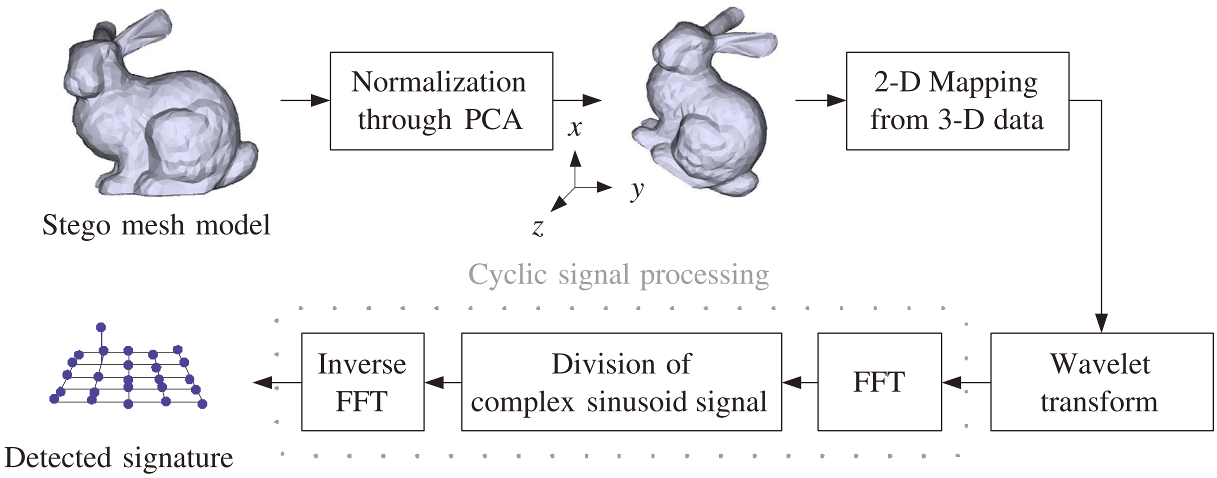

Fig. 3 Block diagram of the watermark extraction for the proposed watermarking method.

3.2 Normalization of 3-D Meshes

Due to rotation, translation, and/or scale operations, vertex coordinates $\mathbf{v}_i = \begin{bmatrix} x_i & y_i & z_i \end{bmatrix}$ $(i = 0, 1, \ldots, V-1)$ of the 3-D mesh is altered without deformation, where V is a number of vertices [12]. In order to align the 3-D mesh in a normalized coordinate system, we utilize a PCA-based method similar to [13], where the PCA is an abbreviation of the principle component analysis. After introducing centered vertices

$$\mathbf{v}'_i = \mathbf{v}_i - \overline{\mathbf{v}}, \quad \overline{\mathbf{v}} = \frac{1}{V}\sum_{i=0}^{V-1}\mathbf{v}_i, \tag{10}$$

we calculate three eigenvectors $\mathbf{c}_t$ $(t = 0, 1, 2)$ with eigenvalues λ_t of a covariance matrix

$$\mathbf{C} = \frac{1}{V}\sum_{i=0}^{V-1}\mathbf{v}'^{T}_i \cdot \mathbf{v}'_i, \tag{11}$$

where $\lambda_0 \geq \lambda_1 \geq \lambda_2$. If the t-th element $\mathbf{c}_t(t)$ of the eigenvector $\mathbf{c}_t$ is negative, we replace $\mathbf{c}_t$ by $-\mathbf{c}_t$, i.e., $\mathbf{c}_t = -\mathbf{c}_t$. We then transform $\mathbf{v}'_i$ into $\mathbf{v}''_i$ in the normalized coordinate system as

$$\mathbf{v}''_i = \begin{bmatrix} x''_i & y''_i & z''_i \end{bmatrix} = \mathbf{v}'_i \cdot \begin{bmatrix} \mathbf{c}_0^T & \mathbf{c}_1^T & \mathbf{c}_2^T \end{bmatrix}. \tag{12}$$

For the normalized vertices $\mathbf{v}''_i$, we add the watermark $w_c(m', n')$ $(c \in \{y, z\},\ m' = 0, 1, \ldots, 2M-1,\ n' = 0, 1, \ldots, 2N-1)$ into y''_i and z''_i in Eq. (12), respectively,

$$\begin{aligned} y_i^{(w)} &= y''_i + g_y \times \\ &\quad w_y\left(\left\lfloor \frac{x''_i - x_{\min}}{X} 2M \right\rfloor, \left\lfloor \frac{\arctan(y''_i/z''_i)}{2\pi} 2N \right\rfloor\right), \\ z_i^{(w)} &= z''_i + g_z \times \\ &\quad w_z\left(\left\lfloor \frac{x''_i - x_{\min}}{X} 2M \right\rfloor, \left\lfloor \frac{\arctan(y''_i/z''_i)}{2\pi} 2N \right\rfloor\right), \end{aligned} \tag{13}$$

where $X = x_{\max} - x_{\min}$ is defined by the maximum $x_{\max}$ and minimum $x_{\min}$ in terms of x''_i, $0 \leq \arctan(y''_i/z''_i) < 2\pi$, and g_y and g_z are scaling factors to provide a tradeoff functionality between imperceptibility and robustness. In Eq. (13), the term $\lfloor \frac{x''_i - x_{\min}}{X} 2M \rfloor$ corresponds approximately to discretized ϕ of vertices $\mathbf{v}''_i$ in the spherical system (r, θ, ϕ), and the another term $\lfloor \frac{\arctan(y''_i/z''_i)}{2\pi} 2N \rfloor$ corresponds to discretized θ of vertices $\mathbf{v}''_i$ in the spherical system (r, θ, ϕ). Since the normalized vertices of real-world 3-D objects are pseudo-uniformly distributed with respect to the axis θ and axis ϕ in the spherical coordinates (r, θ, ϕ), we utilize the two axes for almost evenly inserting the watermark.

The 3-D data constructed by $\begin{bmatrix} x''_i & y_i^{(w)} & z_i^{(w)} \end{bmatrix}$ result in the stego mesh model in Fig. 1.

3.3 Watermark Extraction

Figure 3 illustrates a block diagram of watermark extraction from the watermarked model. In the same manner, the vertices $\tilde{\mathbf{v}}_i = \begin{bmatrix} \tilde{x}_i & \tilde{y}_i & \tilde{z}_i \end{bmatrix}$ $(i = 0, 1, \ldots, V')$ of the stego mesh model are first aligned in the normalized coordinate system. The normalized vertices $\tilde{\mathbf{v}}''_i = \begin{bmatrix} \tilde{x}''_i & \tilde{y}''_i & \tilde{z}''_i \end{bmatrix}$ are mapped to two 2-D data sets $b_y(m', n')$ and $b_z(m', n')$ as

$$\begin{aligned} b_y(m', n') &= \frac{1}{|\mathcal{S}_{m',n'}|}\sum_{i\in\mathcal{S}_{m',n'}} \tilde{y}''_i, \\ b_z(m', n') &= \frac{1}{|\mathcal{S}_{m',n'}|}\sum_{i\in\mathcal{S}_{m',n'}} \tilde{z}''_i, \end{aligned} \tag{14}$$

for $m' = 0, 1, \ldots, 2M-1$ and $n' = 0, 1, \ldots, 2N-1$, where

$$\begin{aligned} \mathcal{S}_{m',n'} = \Bigg\{ i \,\Bigg|\, & \frac{X'}{2M}m' + \tilde{x}_{\min} \leq \tilde{x}''_i < \frac{X'}{2M}(m'+1) \\ & + \tilde{x}_{\min},\ \frac{2\pi}{2N}n' \leq \arctan\left(\frac{\tilde{y}''_i}{\tilde{z}''_i}\right) < \frac{2\pi}{2N}(n'+1) \Bigg\}, \end{aligned} \tag{15}$$

$\tilde{X} = \tilde{x}_{\max} - \tilde{x}_{\min}$ is defined by the maximum $\tilde{x}_{\max}$ and minimum $\tilde{x}_{\min}$ in terms of $\tilde{x}''_i$, and $|\mathcal{S}_{m',n'}|$ denotes the cardinality

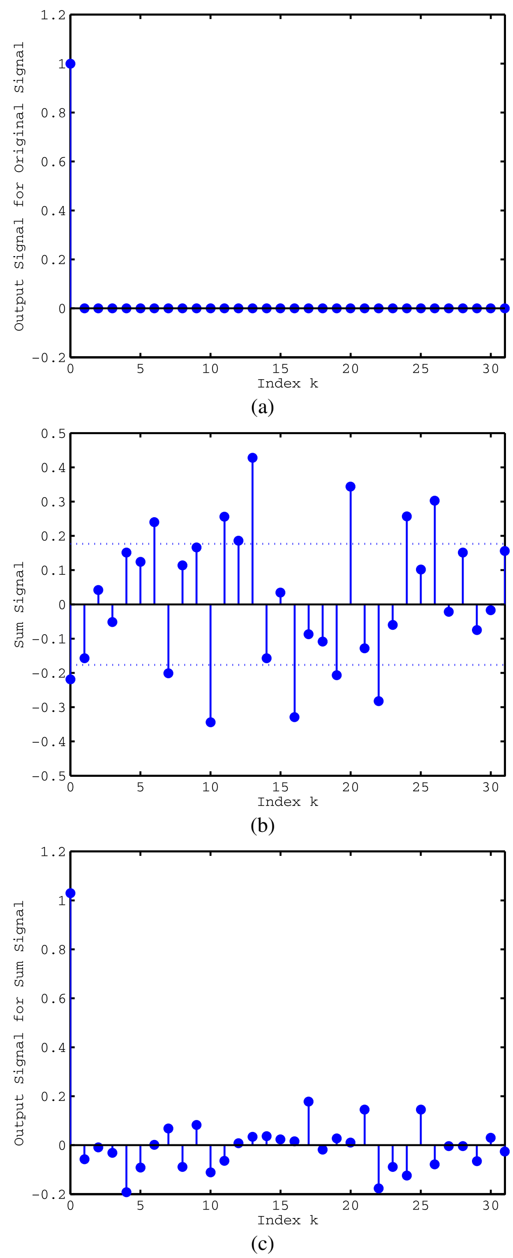

Fig. 4 Example of retrieved signals by the inverse system: (a) output signal $\tilde{s}(k) = s(k)$ for $s'(k)$, (b) sum signal $\tilde{s}'(k)$, and (c) output signal $\tilde{s}(k)$ for $\tilde{s}'(k)$.

of the set $\mathcal{S}_{m',n'}$. These mapped data $b_c(m', n')$ $(c \in \{y, z\})$ are implemented by the Haar wavelet transform and inverse smear transform, denominated desmear transform in [10], respectively,

$$\tilde{s}'_c(m, n) = \frac{1}{2}\{b_c(2m, 2n) - b_c(2m + 1, 2n) \\ -b_c(2m, 2n + 1) + b_c(2m + 1, 2n + 1)\} \tag{16}$$

for $m = 0, 1, \ldots, M - 1$ and $n = 0, 1, \ldots, N - 1$,

$$\tilde{\mathbf{S}}_c = \mathbf{A}'_M \cdot \tilde{\mathbf{S}}'_c \cdot \mathbf{A}'^T_N, \tag{17}$$

$$\mathbf{A}'_K = \frac{1}{K}\mathbf{W}^\dagger_K \cdot \mathbf{D}'_K \cdot \mathbf{W}_K, \tag{18}$$

$$\mathbf{D}'_K = \mathbf{D}^{-1}_K = \mathrm{diag}\left(e^{-j\theta_{0,K}}, e^{-j\theta_{1,K}}, \ldots, e^{-j\theta_{K-1,K}}\right), \tag{19}$$

where $\tilde{\mathbf{S}}_c$ is the output matrix with the (m, n)-th elements $\tilde{s}_c(m, n)$, and $\tilde{\mathbf{S}}'_c$ is the input matrix with the (m, n)-th elements $\tilde{s}'_c(m, n)$. In this paper, if the position index (P'_c, Q'_c) with the maximum value of $\tilde{s}_c(m, n)$ is identical to the signature message (P, Q) in Eq. (1), we determine that the correct watermark is detected. This detection process is equivalent to calculating the correlation between the 2-D signal $\tilde{s}'_c(m, n)$ and spread spectrum code $s'(m, n)$ in Eq. (2). Since the system in Eq. (17) corresponds to the inverse one for Eq. (2), this cyclic signal processing for $s'(k)$ in Eq. (8) reconstructs the impulse signal $\tilde{s}(k) = s(k)$, as shown in Fig. 4 (a). In other words, the sequence in Eq. (2), which is embedded as the watermark in the proposed approach, corresponds to an orthogonal code. For example, when an additive white Gaussian noise $n(k)$ of variance 0.01, i.e, signal to noise ratio 20[dB], is added to $s'(k)$ in Eq. (8), the sum signal $\tilde{s}'(k) = s'(k) + n(k)$ and the output signal $\tilde{s}(k)$ from the inverse system are illustrated in Fig. 4 (b) and Fig. 4 (c), respectively, where

$$\left[\tilde{s}(0) \quad \tilde{s}(1) \quad \cdots \quad \tilde{s}(K-1)\right]^T = \mathbf{A}'_k \cdot \left[\tilde{s}'(0) \quad \tilde{s}'(1) \quad \cdots \quad \tilde{s}'(K-1)\right]^T. \tag{20}$$

From Fig. 4 (c), since the slightly different signal $\tilde{s}(k)$ of the impulse signal $s(k)$ is obtained via the inverse process, we can extract the correct signature message from the degraded signal. In addition to a good correlation property, the merit of the proposed method is relatively low computational complexity due to the FFT.

4. Experimental Results

The performance of the proposed watermarking technique is evaluated for a 3-D semi-regular bunny model with 65538 vertices and 131072 cells as shown in Fig. 5 (a). In the simulations, we used the parameters listed in Table 1 and set $P_c = 15$ and $Q_c = 20$ in Eq. (1) for $c \in \{y, z\}$ as the signature. From the values of M and N, the payload of our watermarking is $2\log_2(MN) = 20$ bits for the case 1 and case 3-5 in Table 1, and $2\log_2(MN) = 24$ bits for the case 2 in Table 1, respectively. The watermarked mesh models of the proposed algorithm for the case 1-4 are displayed in Fig. 5 (b)-(e). For comparison, the watermarked mesh models of the conventional algorithm with a strength coefficient $\gamma = 0.001$ and resolution level $l = 1$ in [14] is also displayed in Fig. 5 (f). In addition, Fig. 6 (a) and (b) show a 3-D irregular Bunny model with 35947 vertices and 69451 cells and the watermarked mesh model, respectively, and Table 1 summarizes the parameters in the case 5 for the irregular model.

The quality of the geometry of the 3-D mesh model

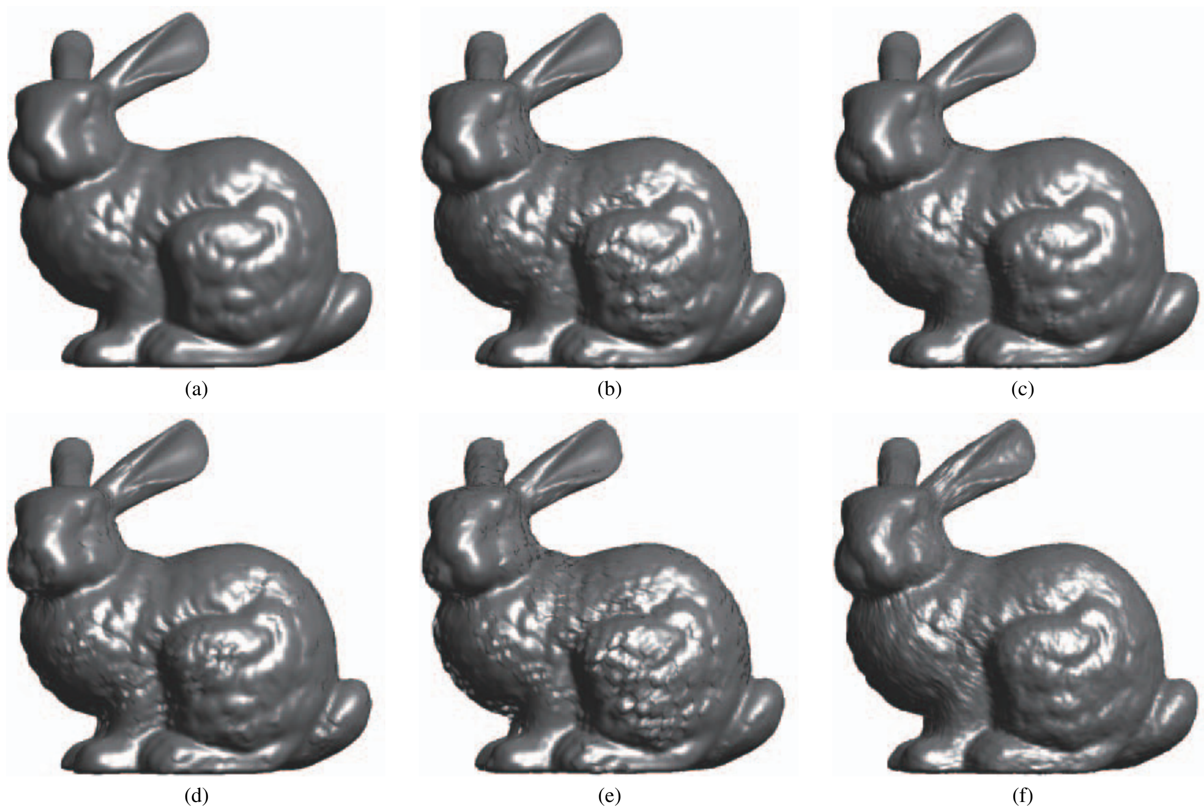

Fig. 5 Semi-regular Bunny models: (a) cover mesh model, (b) stego mesh model via the proposed method (case 1), (c) stego mesh model via the proposed method (case 2), (d) stego mesh model via the proposed method (case 3), (e) stego mesh model via the proposed method (case 4), and (f) stego mesh model via the conventional method in [14].

Table 1 Parameters in the proposed watermarking methods ($c \in \{y, z\}$).

	Size		Spreading factor	Scaling factor	
	M	N	$\alpha_{K,c}$	w_y	w_z
Case 1	32	32	5	0.16	0.08
Case 2	64	64	5	0.16	0.08
Case 3	32	32	10	0.16	0.08
Case 4	32	32	5	0.32	0.16
Case 5	32	32	5	0.08	0.04

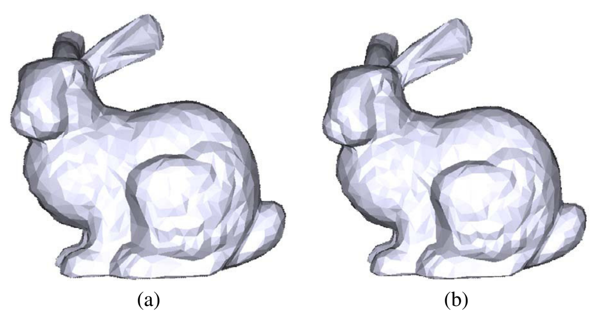

Fig. 6 Irregular Bunny models: (a) cover mesh model and (b) stego mesh model via the proposed method (case 5).

was measured by Metro [20], which provides the forward and backward root mean square (rms) errors, and we used the maximum value of the two rms values. The values of the rms between the cover model in Fig. 5 (a) and the stego model in Fig. 5 (b)-(d) are almost 5×10^{-2}. From both the objective and subjective quality, it can be seen that our watermarking provides only a minor visual degradation. On the other hand, the watermark strength of the case 4 is enhanced according to scaling factors w_y, w_z in Table 1. Compared with the original mesh, the modifications in the watermarked model can be noticed, and the value of the rms between the cover model in Fig. 5 (a) and the stego model in Fig. 5 (e) results in 1.2×10^{-1}.

To assess the robustness of the watermark, we construct 100 stego models rotated, translated, scaled, and attacked by additive white Gaussian noise with standard variation σ in the range $0 \leq \sigma \leq 0.004$. The ratios of detecting the correct message are tabulated in Table 2 for the semi-regular model in Fig. 5 (a) and Table 3 for the irregular model in Fig. 6 (a), respectively.

It is seen from Table 2 and Table 3 that the proposed method can extract the correct message against rotation and translation, scale conversion, additive noise. Particularly from the results of the standard variation $\sigma = 0$ in these tables, one can observe that the normalization procedure in the proposed method is robust to the geometric manipulations. Comparing the case 1 and case 3 in Fig. 5 and Table 2, it is seen that the spreading factor $\alpha_{K,c}$ does not significantly affect the performance. In addition, it is seen from these tables

Table 2 Ratios of detecting the correct message from rotated, translated, scaled, and attacked 3-D models for the semi-regular model.

Standard variation σ ($\times 10^{-3}$)	0	0.5	1.0	2.0	4.0
Proposed method					
Case 1	1.00	0.96	0.88	0.76	0.54
Case 2	1.00	0.76	0.59	0.30	0.04
Case 3	1.00	0.95	0.85	0.77	0.52
Case 4	1.00	1.00	0.97	0.90	0.80
Conventional method in [14]	1.00	0.58	0.24	0.13	0.03

Table 3 Ratios of detecting the correct message from rotated, translated, scaled, and attacked 3-D models for the irregular model.

Standard variation σ ($\times 10^{-3}$)	0	0.5	1.0	2.0	4.0
Case 5	1.00	1.00	1.00	0.91	0.58

that the ratio results degrade as the noise strength increases. The experimental results in Fig. 5 and Table 2 demonstrate the superiority of the proposed watermarking method over the conventional watermarking method in [14]. On the other hand, it is worth noting that the watermarking algorithm in [14] is not applied to the irregular model in Fig. 6 (a) and the results of [14] are omitted in Fig. 6 and Table 3.

5. Conclusions

In this paper, we presented a correlation-based watermarking algorithm with cyclic signal processing for 3-D polygonal meshes. The proposed scheme differs from the algorithms with the pseudo-random sequence in that our watermark is generated from the impulse signal via cyclic signal processing. This watermark leads to a good performance in terms of robustness and perceptual transparency, because of the property of the orthogonal code. Experimental results show the validity of the proposed technique in 3-D watermarking for some common alterations such as rotation and noise addition.

Acknowledgment

This work was supported in part by Grant-in-Aid for Scientific Research (21760296) from the Japan Society for the Promotion of Science.

References

[1] F. Hartung and M. Kutter, "Multimedia watermarking techniques," Proc. IEEE, vol.87, pp.1079–1107, July 1999.
[2] I.J. Cox, M.L. Miller, and J.A. Bloom, Digital Watermarking, San Mateo, Morgan Kaufman, CA, 2001.
[3] C.I. Podilchuk and E.J. Delp, "Digital watermarking: Algorithms and applications," IEEE Signal Process. Mag., vol.18, no.4, pp.33–46, July 2001.
[4] I.J. Cox, J. Kilian, F.T. Leighton, and T. Shamoon, "Secure spread spectrum watermarking for multimedia," IEEE Trans. Image Process., vol.6, no.12, pp.1673–1687, Dec. 1997.
[5] B. Chen and G. Wornell, "Quantization index modulation: A class of provably good methods for digital watermarking and information embedding," IEEE Trans. Inf. Theory, vol.47, no.4, pp.1423–1443, May 2001.
[6] R. Obuchi, H. Masuda, and M. Aono, "Watermarking three-dimensional polygonal models through geometric and topological modifications," IEEE J. Sel. Areas Commun., vol.16, no.4, pp.551–560, May 1998.
[7] E. Praun, H. Hoppe, and A. Finkelstein, "Robust mesh watermarking," Proc. ACM SIGGRAPH, pp.69–76, Aug. 1999.
[8] Z.Q. Yu, H.H.S. Ip, and L.F. Kwork, "A robust watermarking scheme for 3D triangle mesh models," Pattern Recognit., vol.36, pp.2603–2614, 2003.
[9] F. Cayre and B. Macq, "Data hiding on 3-D triangle meshes," IEEE Trans. Signal Process., vol.51, no.4, pp.939–949, April 2003.
[10] T. Okahisa and K. Ohue, "Smearing-desmearing transformation and the application to digital watermark," Proc. SPIE, vol.3971, pp.110–117, May 2000.
[11] P.P. Vaidyanathan and A. Kiraç, "Cyclic LTI systems in digital signal processing," IEEE Trans. Signal Process., vol.47, no.2, pp.433–447, Feb. 1999.
[12] Gabriele Lohmann, Volumetric Image Analysis, Chichester, Wiley-Teubner, NY, 1998.
[13] M. Elad, A. Tal, and S. Ar, "Directed search in a 3D objects database using SVM," HP Laboratories Israel Technical Report, HPL-2000-20 (R.1), Aug. 2000.
[14] F. Uccheddu, M. Corsini, and M. Barni, "Wavelet-based blind watermarking of 3D models," Proc. ACM Int. Workshop Multimedia and Security, pp.143–154, Sept. 2004.
[15] S. Kanai, H. Date, and T. Kishinami, "Digital watermarking for 3D polygons using multiresolution wavelet decomposition," Proc. Sixth IFIT WG5.2 Geo-6, pp.296–307, Dec. 1998.
[16] O. Benedens, "Two high capacity methods for embedding public watermarks into 3D polygonal models," Proc. ACM Int. Workshop Multimedia and Security, pp.95–99, Oct. 1999.
[17] M. Eck, T. DeRose, T. Duchamp, H. Hoppe, M. Lounsbery, and W. Stuetzle, "Multiresolution analysis of arbitrary meshes," Proc. ACM SIGGRAPH, pp.173–182, Aug. 1995.
[18] X. Gu, S. Gortler, and H. Hoppe, "Geometry images," Proc. ACM SIGGRAPH, pp.355–361, July 2002.
[19] I. Guskov, "Manifold-based approach to semi-regular remeshing," Graphical Models, vol.69, pp.1–18, Jan. 2007.
[20] P. Cignoni, C. Rocchini, and R. Scopigno, "Metro: Measuring error on simplified surfaces," Comput. Graph. Forum, vol.17, pp.167–174, June 1998.

Toshiyuki Uto received the B.E., M.E., and Ph.D. degrees from the Department of Electrical Engineering, Keio University, Yokohama, Japan, in 1999, 2001, and 2004, respectively. Since 2004, he has been with the Ehime University, Matsuyama, Japan, where he is currently a Senior Assistant Professor with the Department of Computer Science. His research interests include digital signal processing and multirate systems, and 3-D image processing.

Yuka Takemura received the B.E. degree from the Department of Computer Science, Ehime University, Matsuyama, Japan, in 2007. Since 2007, she has been with the Ube Information Systems, Ube, Yamaguchi, Japan. Her research interests include digital watermarking and 3-D image processing.

Hidekazu Kamitani received the B.E. degree from the Department of Computer Science, Ehime University, Matsuyama, Japan, in 2007, and currently pursuing the M.E. degree at the same institution. His research interests include digital signal processing and digital communications.

Kenji Ohue received the B.E. degree from Ehime University, Matsuyama, Japan, in 1970, the M.E. degree from Osaka Prefecture University, Osaka, Japan, in 1972, and the Ph.D. degree from Tohoku University, Sendai, Japan, in 1988, respectively. In 1972, he joined the Nippon Telegraph and Telephone Corporation. Since 1989, he has been working with the Ehime University, Matsuyama, Japan, where he is currently a Professor with the Department of Computer Science. His research interests are in the areas of digital transmission system, code theory, and information security.